Uncertainties in the Charm Production Cross Section

R. Vogt

Lawrence Livermore National Laboratory, Livermore, CA 94551, USA

Physics Department, University of California, Davis, CA 95616, USA

Calculating Heavy Flavors in Perturbative QCD

'Hard' processes have a large scale in the calculation that makes perturbative QCD applicable: high momentum transfer, μ^2, high mass, m, high transverse momentum, p_T, since $m \neq 0$, heavy quark production is a 'hard' process

Asymptotic freedom assumed to calculate the interactions between two hadrons on the quark/gluon level but the confinement scale determines the probability of finding the interacting parton in the initial hadron

Factorization assumed between perturbative, calculable hard scattering and the universal, nonperturbative parton distribution functions

Hadronic cross section in an AB collision where $AB = pp, pA$ or nucleus-nucleus is

$$\sigma_{AB}(S, m^2) \;=\; \sum_{i,j=q,\overline{q},g} \int_{4m_Q^2/s}^{1} \frac{d\tau}{\tau} \int dx_1\, dx_2\, \delta(x_1 x_2 - \tau) f_i^A(x_1, \mu_F^2)\, f_j^B(x_2, \mu_F^2)\, \widehat{\sigma}_{ij}(s, m^2, \mu_F^2, \mu_R^2)$$

f_i^A are nonperturbative parton distributions, determined from global fits, x_1, x_2 are momentum fraction of A and B carried by partons i and j, $\tau = s/S$

$\widehat{\sigma}_{ij}(s, m^2, \mu_F^2, \mu_R^2)$ is hard partonic cross section calculable in QCD in powers of α_s^{2+n}: leading order (LO), $n = 0$; next-to-leading order (NLO), $n = 1$ ...

Number of light flavors in α_s based on mass scale: $n_{\rm lf} = 3$ for c and 4 for b

Results depend strongly on quark mass, m, factorization scale, μ_F, in the parton densities and renormalization scale, μ_R, in α_s

Total Cross Sections

Partonic total cross section only depends on quark mass m, not kinematics
To NLO

$$\begin{aligned}\widehat{\sigma}_{ij}(s,m,\mu_F^2,\mu_R^2) &= \frac{\alpha_s^2(\mu_R^2)}{m^2}\Big\{f_{ij}^{(0,0)}(\rho) \\ &+ 4\pi\alpha_s(\mu_R^2)\Big[f_{ij}^{(1,0)}(\rho)+f_{ij}^{(1,1)}(\rho)\ln(\mu_F^2/m^2)\Big]+\mathcal{O}(\alpha_s^2)\Big\}\end{aligned}$$

$\rho = 4m^2/s$, s is partonic center of mass energy squared

μ_F is factorization scale, separates hard part from nonperturbative part

μ_R is renormalization scale, scale at which strong coupling constant α_s is evaluated

$\mu_F = \mu_R$ in evaluations of parton densities

$f_{ij}^{(a,b)}$ are dimensionless, μ-independent scaling functions, $a=0$, $b=0$ and $ij = q\overline{q}$, gg for LO, $a=1$, $b=0,1$ and $ij = q\overline{q}$, gg and qg, $\overline{q}g$ for NLO

$f_{ij}^{(0,0)}$ are always positive, $f_{ij}^{(1,b)}$ can be negative also

Note that if $\mu_F^2 = m^2$, $f_{ij}^{(1,1)}$ does not contribute

Scaling Functions to NLO

Near threshold, $\sqrt{s}/2m \to 1$, Born contribution is large but dies away for $\sqrt{s}/2m \to \infty$

At large $\sqrt{s}/2m$, gg channel is dominant, then qg

NLO gg and qg scaling functions independent of energy at $\sqrt{s}/2m > 20$

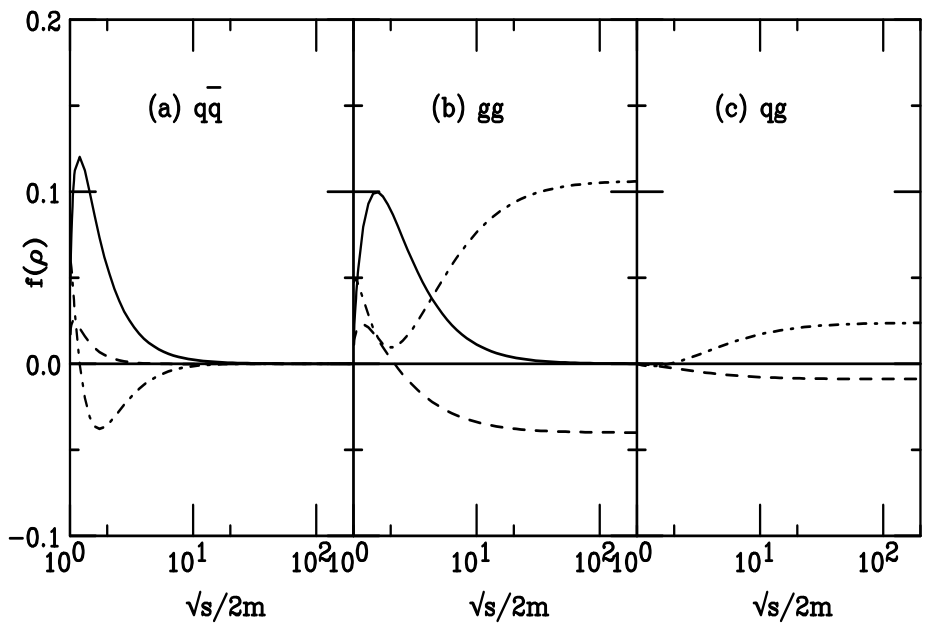

Figure 1: Scaling functions needed to calculate the total partonic $Q\overline{Q}$ cross section. The solid curves are the Born results, $f_{ij}^{(0,0)}$, the dashed and dot-dashed curves are NLO contributions, $f_{ij}^{(1,1)}$ and $f_{ij}^{(1,0)}$ respectively.

Some Diagrams Contributing to NLO Heavy Flavor Production

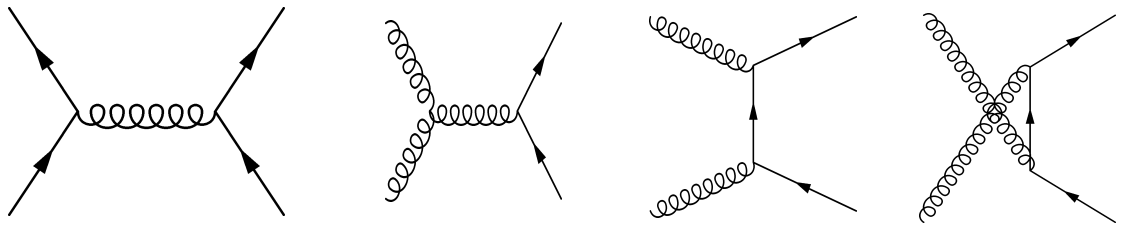

Figure 2: Leading order processes contributing to $Q\overline{Q}$ production.

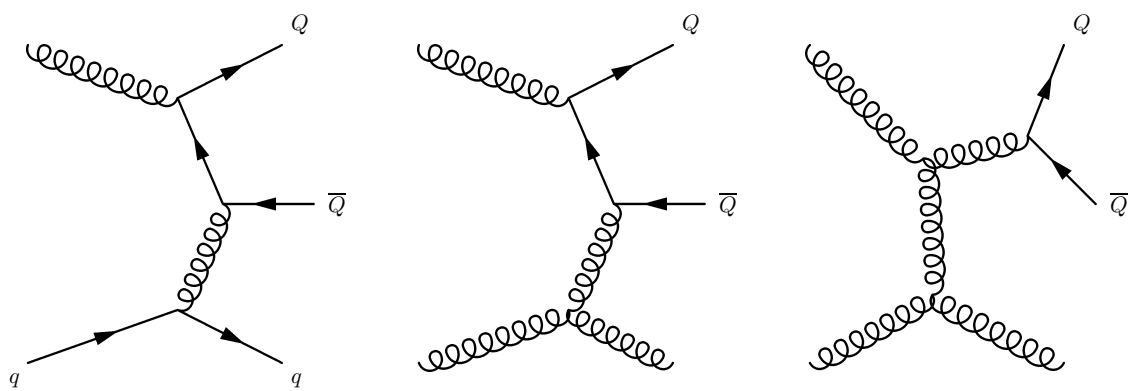

Figure 3: Examples of next-to-leading order diagrams contributing to $Q\overline{Q}$ production: $qg \to qQ\overline{Q}$ (left) and $gg \to Q\overline{Q}g$ (middle and right).

Choosing Parameters

Two important parameters: the quark mass m and the scale μ – at high energies, far from threshold, the low x, low μ behavior of the parton densities determines the charm result, bottom less sensitive to parameter choice

CTEQ6M Minimum scale $\mu_{\rm min} = 1.3$ GeV, $\Lambda_{\rm QCD}^{n_f=5} = 0.226$ GeV, large α_s for charm scales;

GRV98 Older set, lower minimum scale $\mu_{\rm min} = 0.89$ GeV, lower $\Lambda_{\rm QCD}^{n_f=5} = 0.1677$ GeV, lower α_s for charm.

The scale is usually chosen so that $\mu_F = \mu_R$, as in parton density fits, no strict reason for doing so for heavy flavors

Two ways to make predictions:

Fit to Data (Hard Probes Collaboration): fix m and $\mu \equiv \mu_F = \mu_R \geq m$ to data at lower energies and extrapolate to unknown regions – favors lower m;

Uncertainty Band (Cacciari, Nason and RV): band determined from mass range, $1.3 < m < 1.7$ GeV (charm) and $4.5 < m < 5$ GeV (bottom) with $\mu_F = \mu_R = m$, and range of scales relative to central mass value, $m = 1.5$ GeV (charm) and 4.75 GeV (bottom): $(\mu_F/m, \mu_R/m) = (1,1)$, (2,2), (0.5,0.5), (0.5,1), (1,0.5), (1,2), (2,1).

Charm Production as a Function of m and μ^2

Keeping $\mu_F^2 = \mu_R^2 = \mu^2$, as in parton density fits ($\mu < m$ not shown)

The pp data are from reviews by Tavernier (1987), Appel (1992) and later

More recent data favors lower masses

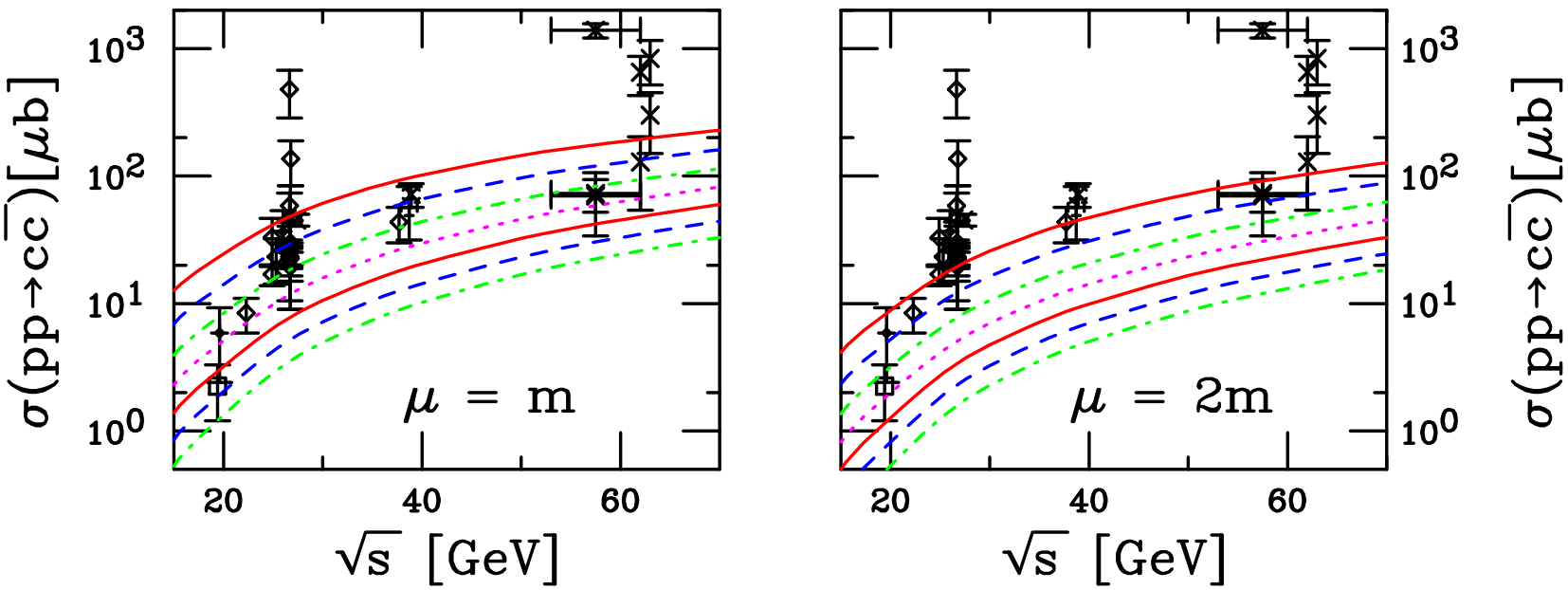

Figure 4: Total $c\bar{c}$ cross sections in pp interactions up to ISR energies as a function of the charm quark mass. All calculations are fully NLO using the CTEQ6M parton densities. The left-hand plot shows the results with the $\mu_R = \mu_F = m$ while in the right-hand plot $\mu_R = \mu_F = 2m$. From top to bottom the curves are $m = 1.2$, 1.3, 1.4, 1.5, 1.6, 1.7, and 1.8 GeV.

Extrapolation to Higher Energies

Large $\sqrt{S}$ behavior of $c\bar{c}$ cross section due to low x behavior of PDFs and phase space – lower scale closer to minimum μ of PDFs, strong factorization scale dependence of gluon density at low μ

Only most recent measurements shown, including the PHENIX $\sqrt{S} = 130$ and 200 GeV (Au+Au and pp respectively) results and STAR pp and d+Au points at $\sqrt{S} = 200$ GeV

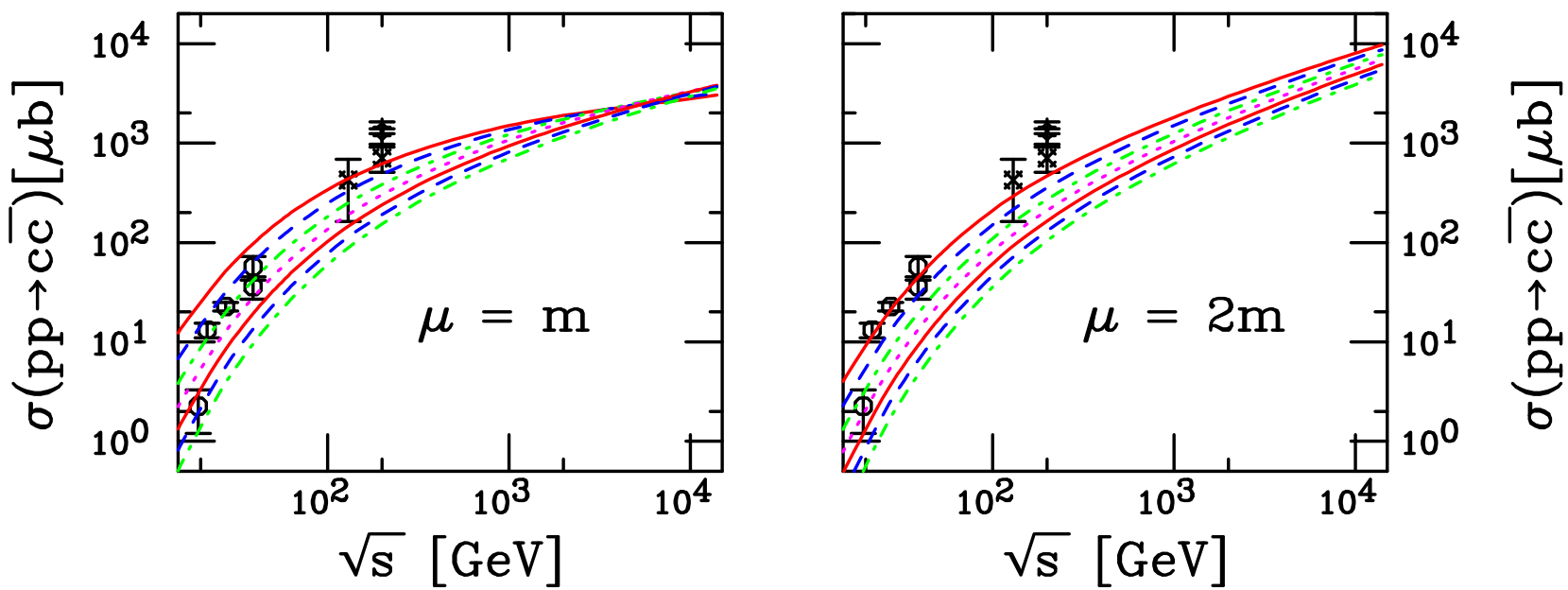

Figure 5: Total $c\bar{c}$ cross sections in pp interactions up to 14 TeV with the CTEQ6M PDFs. The left-hand plot shows the results with the $\mu_R = \mu_F = m$ while in the right-hand plot $\mu_R = \mu_F = 2m$. From top to bottom the curves are $m = 1.2$, 1.3, 1.4, 1.5, 1.6, 1.7, and 1.8 GeV

CTEQ6M Gluon Distributions at Low x and Scale

Backwards evolution required for low scale ($\mu = m,\ m/2$) charm production
At RHIC energies and higher, the low scale gluon distribution turns over

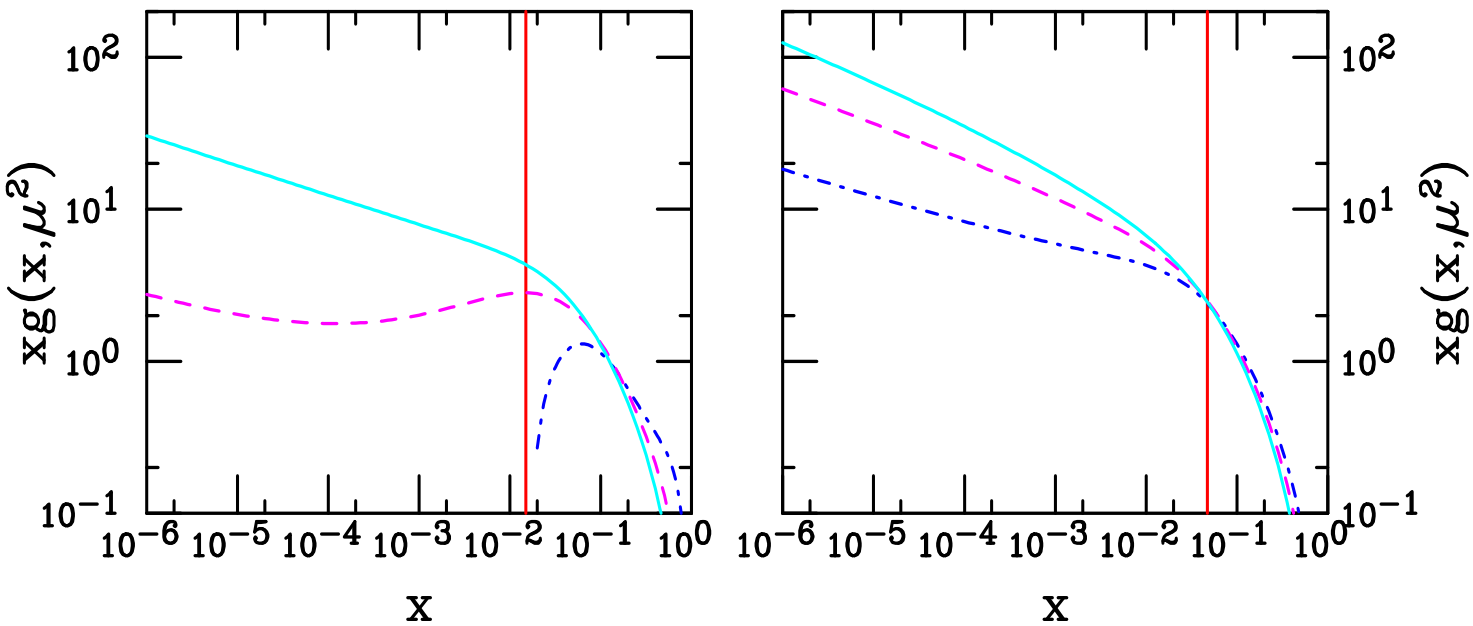

Figure 6: The CTEQ6M parton densities as a function of x for $\xi = 0.5$ (dot-dashed), $\xi = 1$ (dashed) and $\xi = 2$ (solid) for $m = 1.5$ GeV (left-hand side) and 4.75 GeV (right-hand side). The vertical line is the value $x = 2m/\sqrt{s}$ in $\sqrt{s} = 200$ GeV pp collisions at RHIC.

Charm Theoretical Uncertainty: CTEQ6M

Uncertainty band (Cacciari, Nason and RV): from mass range $1.3 < m < 1.7$ **GeV with** $\mu_F = \mu_R = m$**, and scale range relative to central mass value,** $m = 1.5$ **GeV –** $(\mu_F/m, \mu_R/m) = (1,1)$**, (2,2), (0.5,0.5), (0.5,1), (1,0.5), (1,2), (2,1)**

$(\mu_F/m, \mu_R/m) = (1, 0.5)$ **and (0.5,0.5) have large** σ **at** $\sqrt{S} < 100$ **GeV since** α_s **big**

At large $\sqrt{S}$ $(\mu_F/m, \mu_R/m) = (0.5, 0.5)$**, (0.5,1) flattens because** $\mu_F < \mu_0$ **of PDF**

Evolution faster for combination of small x **and high** μ $[(\mu_F/m, \mu_R/m) = (2, 2)$**, (2,1)]**

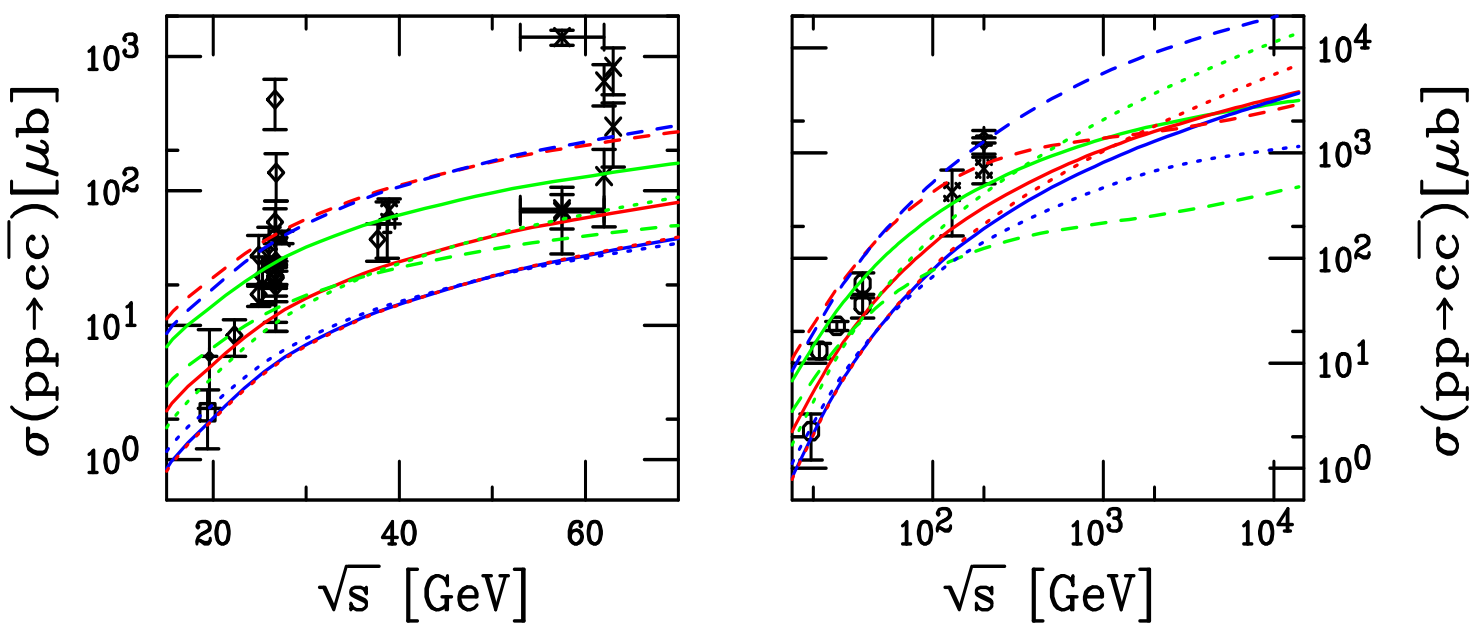

Figure 7: Total $c\bar{c}$ cross sections calculated using CTEQ6M. The solid red curve is the central value $(\mu_F/m, \mu_R/m) = (1,1)$ with $m = 1.5$ GeV. The green and blue solid curves are $m = 1.3$ and 1.7 GeV with (1,1) respectively. The red, blue and green dashed curves correspond to (0.5,0.5), (1,0.5) and (0.5,1) while the red, blue and green dotted curves are for (2,2), (1,2) and (2,1), all for $m = 1.5$ GeV.

Uncertainty Bands for the Total Cross Section

Due to range of parameters chosen for uncertainty band, the maximum and minimum result as a function of energy may not come from a single set of parameters

Thus the upper and lower curves in the band do not represent a single set of μ_R, μ_F and m values but are the upper and lower limits of mass and scale uncertainties added in quadrature:

$$\sigma_{\rm max} = \sigma_{\rm cent} + \sqrt{(\sigma_{\mu,\rm max} - \sigma_{\rm cent})^2 + (\sigma_{m,\rm max} - \sigma_{\rm cent})^2}$$

$$\sigma_{\rm min} = \sigma_{\rm cent} - \sqrt{(\sigma_{\mu,\rm min} - \sigma_{\rm cent})^2 + (\sigma_{m,\rm min} - \sigma_{\rm cent})^2}$$

The central values are $m = 1.5$ GeV (charm) and 4.75 GeV (bottom), $\mu_F = \mu_R = m$

Previous (HPC) charm 'fits' with $m = 1.2$ GeV, $\mu_F = \mu_R = 2m$ fall within the uncertainty band

Charm Uncertainty Band: CTEQ6M

Charm uncertainty larger for $n_{\rm lf} = 3$ than for FONLL calculation based on integrating p_T distribution where charm is active light flavor at high p_T

Biggest effect due to number of light flavors

$$\sigma_{c\bar{c}}^{\rm NLO_{n_{lf}}} = 301^{+1000}_{-210}\ \mu{\rm b} \text{ at } \sqrt{S} = 200 \text{ GeV}$$

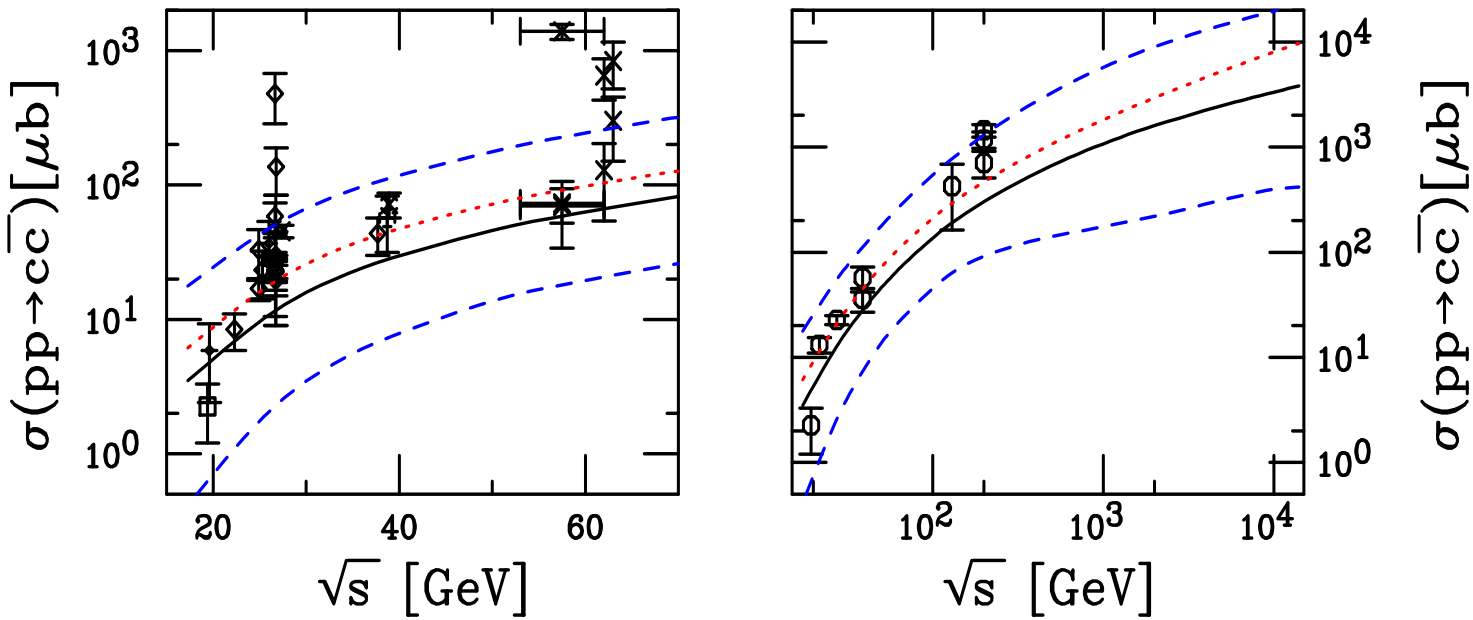

Figure 8: The NLO total $c\bar{c}$ cross sections as a function of $\sqrt{s}$ for $\sqrt{s} \leq 70$ GeV (left-hand side) and up to 14 TeV (right-hand side) calculated with the CTEQ6M parton densities. The solid curve is the central result; the upper and lower dashed curves are the upper and lower edges of the uncertainty band. The dotted curves are calculations with $m = 1.2$ GeV, $\mu_F = \mu_R = 2m$.

Bottom Theoretical Uncertainty: CTEQ6M

Band narrower for higher mass bottom, $\mu_F/m = 0.5$ not near initial PDF scale

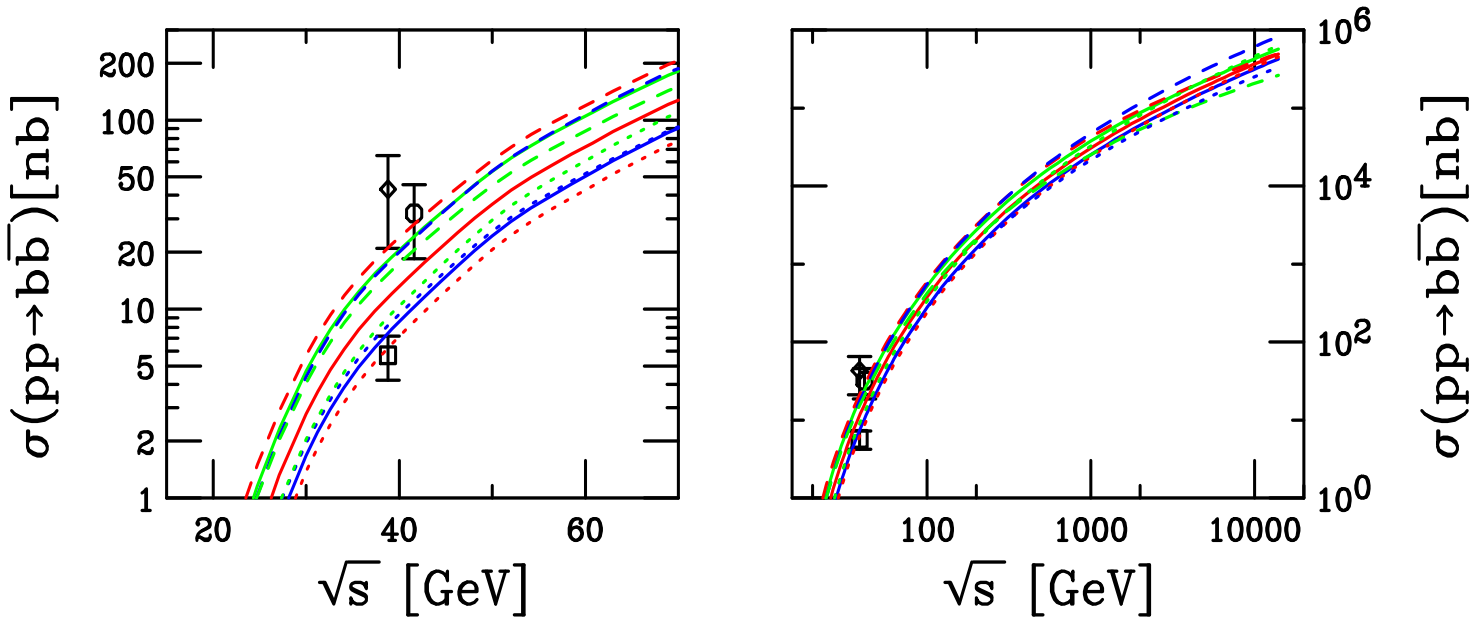

Figure 9: Total $b\bar{b}$ cross sections calculated using CTEQ6M. The solid red curve is the central value $(\mu_F/m, \mu_R/m) = (1,1)$ with $m = 4.75$ GeV. The green and blue solid curves are $m = 4.5$ and 5 GeV with (1,1) respectively. The red, blue and green dashed curves correspond to (0.5,0.5), (1,0.5) and (0.5,1) respectively while the red, blue and green dotted curves are for (2,2), (1,2) and (2,1) respectively, all for $m = 4.75$ GeV.

Bottom Uncertainty Band: CTEQ6M

Low x and scale behavior of gluon density does not affect bottom production since $m_b/2 > m_c$

$$\sigma_{b\bar{b}}^{\mathrm{NLO_{n_{lf}}}} = 2.06^{+1.25}_{-0.81}\ \mu\mathrm{b} \text{ at } \sqrt{S} = 200 \text{ GeV}$$

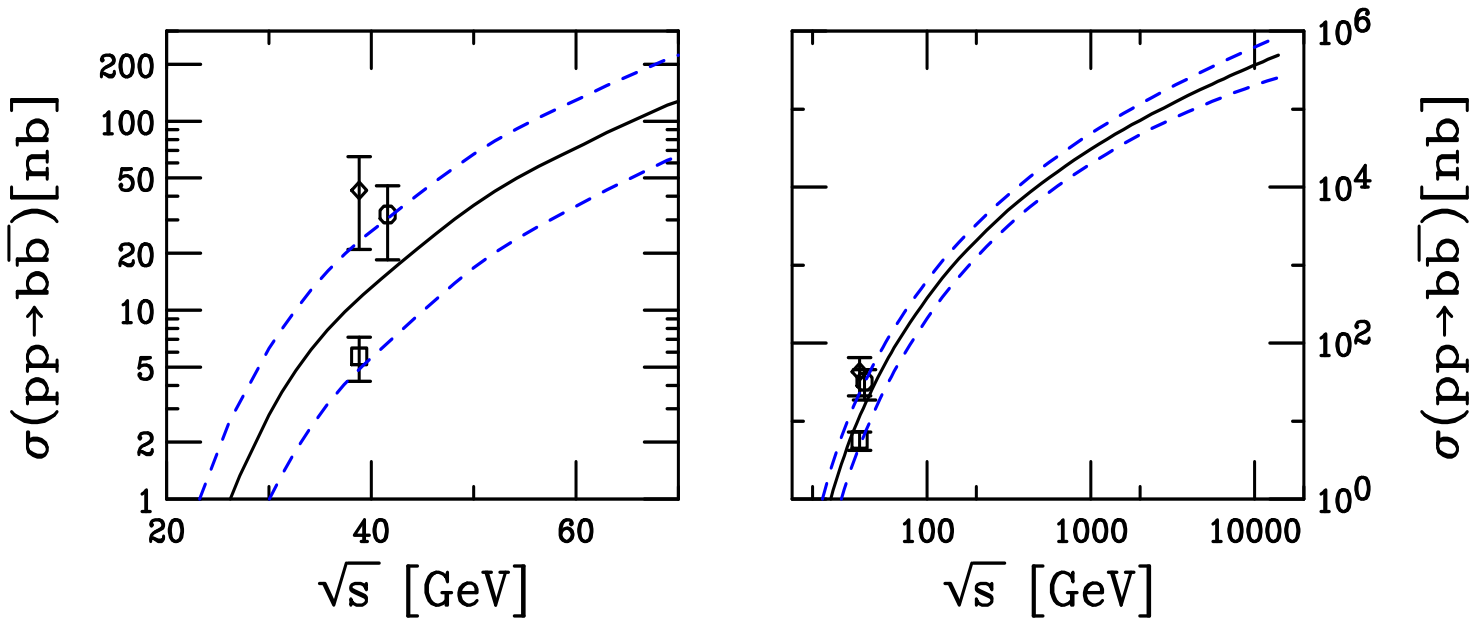

Figure 10: The NLO total $b\bar{b}$ cross sections as a function of $\sqrt{s}$ for $\sqrt{s} \leq 70$ GeV (left-hand side) and up to 14 TeV (right-hand side) calculated with the CTEQ6M parton densities. The solid curve is the central result; the upper and lower dashed curves are the upper and lower edges of the uncertainty band.

GRV98 Gluon Distributions at Low x and Scale

Starts at lower scales than CTEQ6M and MRST sets thus less backwards evolution needed

$xg(x, \mu^2)$ never becomes negative for charm production

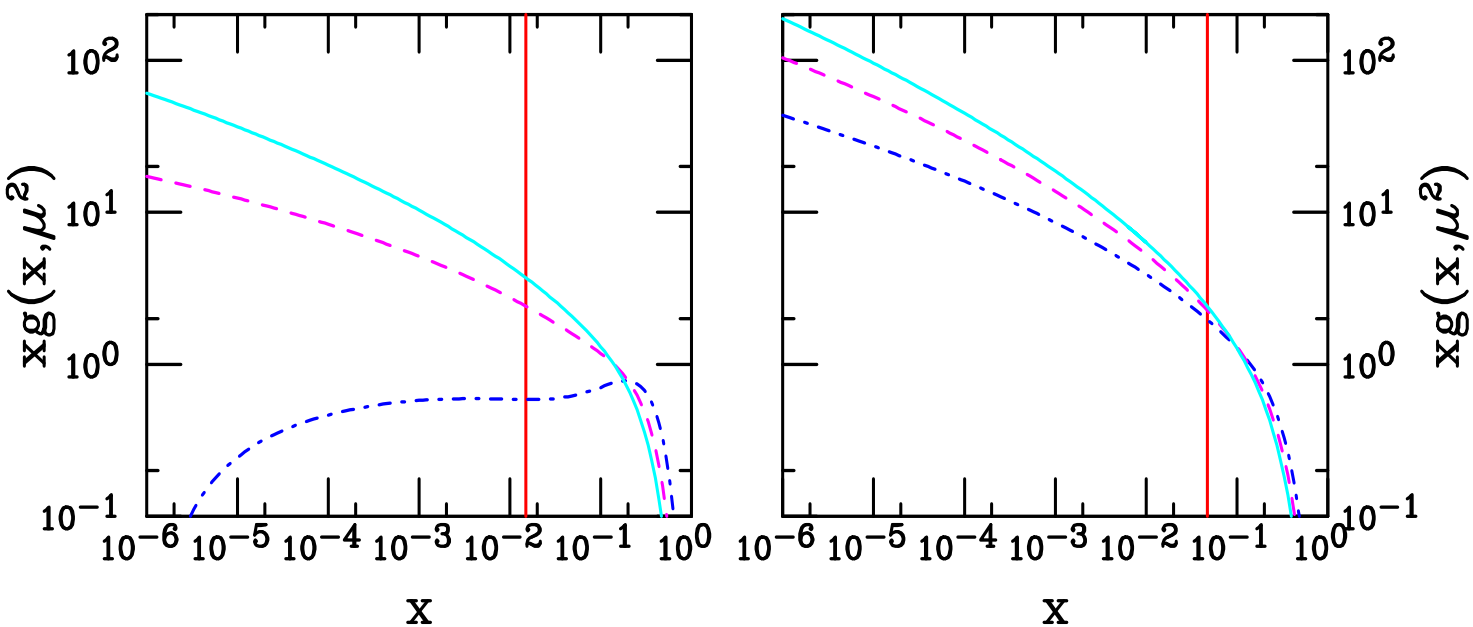

Figure 11: The GRV98 parton densities as a function of x for $\xi = 0.5$ (dot-dashed), $\xi = 1$ (dashed) and $\xi = 2$ (solid) for $m = 1.5$ GeV (left-hand side) and 4.75 GeV (right-hand side). The vertical line is the value $x = 2m/\sqrt{s}$ in $\sqrt{s} = 200$ GeV pp collisions at RHIC.

Charm Theoretical Uncertainty: GRV98

Uncertainty band (Cacciari, Nason and RV): from mass range $1.3 < m < 1.7$ GeV with $\mu_F = \mu_R = m$, and scale range relative to central mass value, $m = 1.5$ GeV – $(\mu_F/m, \mu_R/m) = (1,1)$, (2,2), (0.5,0.5), (0.5,1), (1,0.5), (1,2), (2,1)

Similar behavior as with CTEQ6M but the mass and scale combinations do not result is as wide a range, cross sections are all smaller than CTEQ6M

Turnover for $\mu_F/m = 0.5$ less abrupt than with CTEQ6M

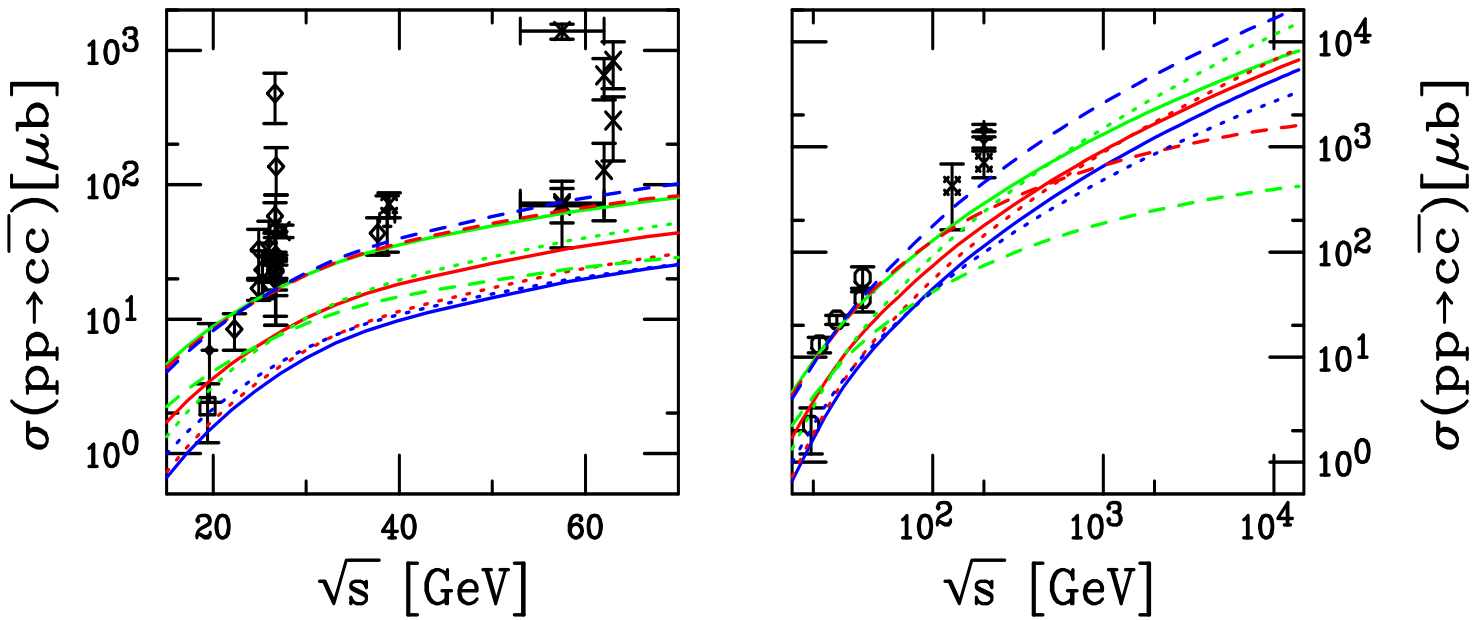

Figure 12: Total $c\bar{c}$ cross sections calculated using GRV98. The solid red curve is the central value $(\mu_F/m, \mu_R/m) = (1,1)$ with $m = 1.5$ GeV. The green and blue solid curves are $m = 1.3$ and 1.7 GeV with (1,1) respectively. The red, blue and green dashed curves correspond to (0.5,0.5), (1,0.5) and (0.5,1) while the red, blue and green dotted curves are for (2,2), (1,2) and (2,1), all for $m = 1.5$ GeV.

Charm Uncertainty Band: GRV98

Lower value of $\Lambda_{\rm QCD}$ gives a smaller two-loop value of α_s than CTEQ6M so that the upper limit of the band is lower for GRV98

$$\sigma_{c\bar{c}}^{\rm NLO_{n_{lf}}} = 178^{+300}_{-122}\ \mu{\rm b} \text{ at } \sqrt{S} = 200 \text{ GeV}$$

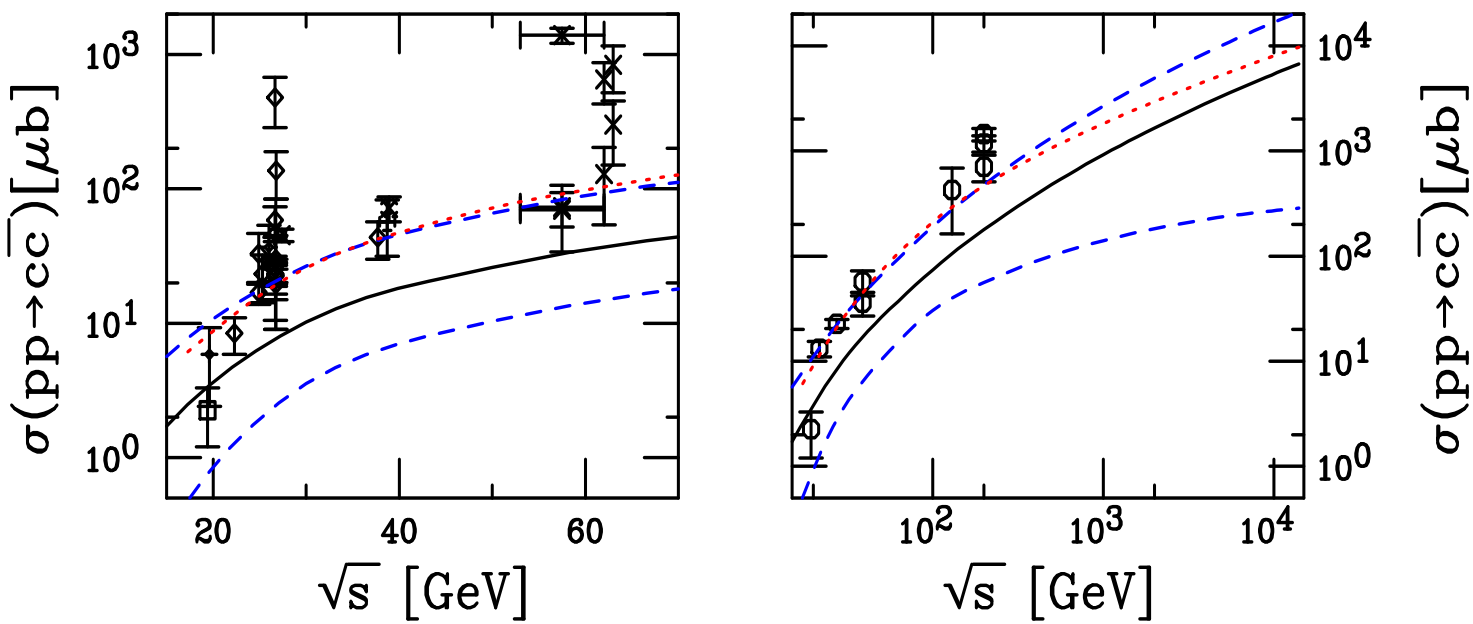

Figure 13: The NLO total $c\bar{c}$ cross sections as a function of $\sqrt{s}$ for $\sqrt{s} \leq 70$ GeV (left-hand side) and up to 14 TeV (right-hand side) calculated with the GRV98 parton densities. The solid curve is the central result; the upper and lower dashed curves are the upper and lower edges of the uncertainty band. The dotted curves are calculations with $m = 1.2$ GeV, $\mu_F = \mu_R = 2m$.

Bottom Theoretical Uncertainty: GRV98

Less difference between parton densities for bottom than for charm

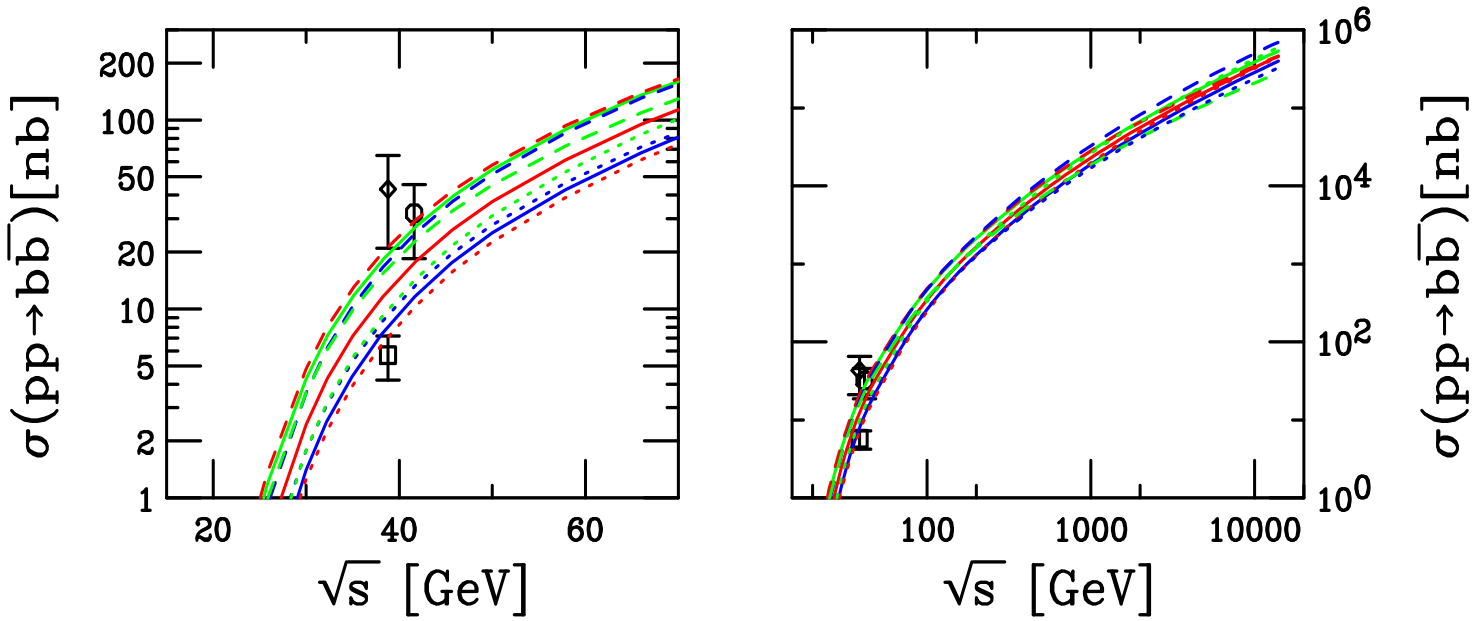

Figure 14: Total $b\bar{b}$ cross sections calculated using GRV98. The solid red curve is the central value $(\mu_F/m, \mu_R/m) = (1,1)$ with $m = 4.75$ GeV. The green and blue solid curves are $m = 4.5$ and 5 GeV with (1,1) respectively. The red, blue and green dashed curves correspond to (0.5,0.5), (1,0.5) and (0.5,1) respectively while the red, blue and green dotted curves are for (2,2), (1,2) and (2,1) respectively, all for $m = 4.75$ GeV.

Bottom Uncertainty Band: GRV98

Bottom uncertainty similar to that for CTEQ6M, less sensitive to parton distribution due to larger scale

Biggest effect due to number of light flavors

$$\sigma_{b\bar{b}}^{\mathrm{NLO}_{\mathrm{n_{lf}}}} = 1.65^{+0.77}_{-0.53}\ \mu\mathrm{b} \text{ at } \sqrt{S} = 200 \text{ GeV}$$

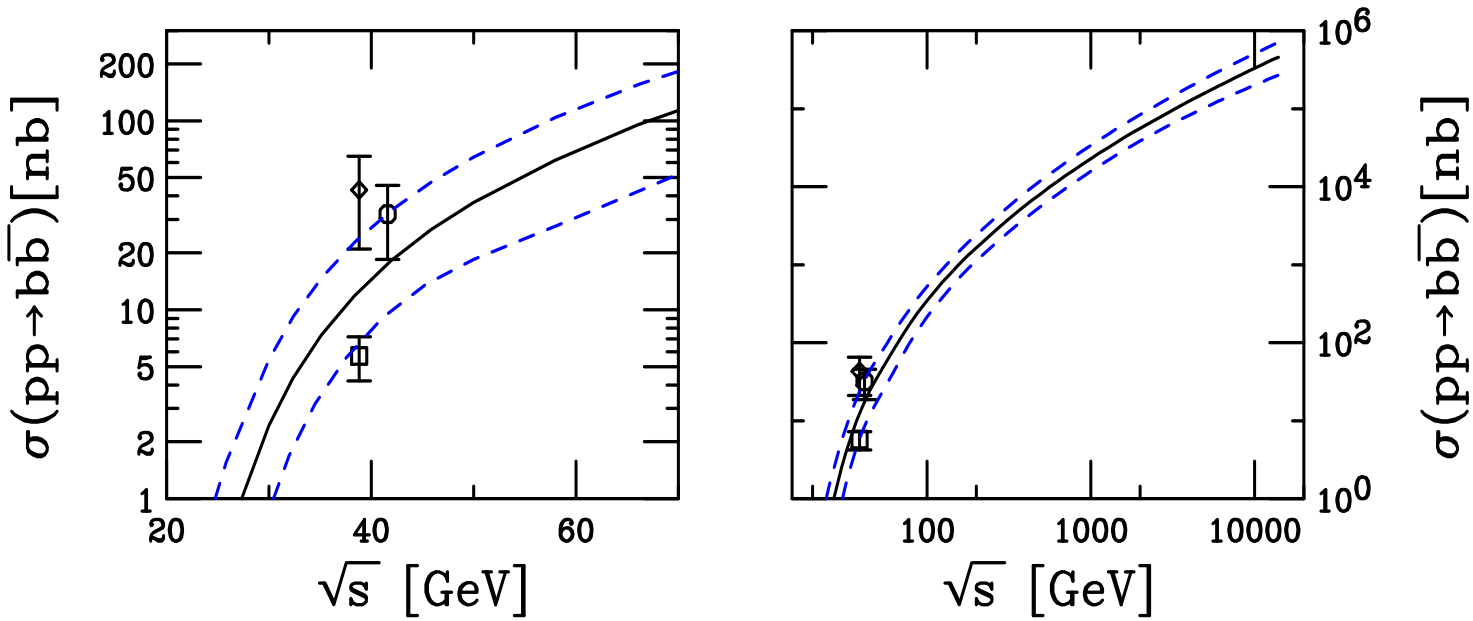

Figure 15: The NLO total $b\bar{b}$ cross sections as a function of $\sqrt{s}$ for $\sqrt{s} \leq 70$ GeV (left-hand side) and up to 14 TeV (right-hand side) calculated with the CTEQ6M parton densities. The solid curve is the central result; the upper and lower dashed curves are the upper and lower edges of the uncertainty band. The dotted curves are calculations with $m = 1.2$ GeV, $\mu_F = \mu_R = 2m$.

Differences Between CTEQ6M and GRV98

Smaller GRV98 $\Lambda_{\rm QCD}^{n_f=5}$ gives larger $\mu_R/\Lambda_{\rm QCD}^{n_f=5}$ ratio, lowering α_s for GRV98, reducing the $\alpha_s(\xi_R=0.5)/\alpha_s(\xi_R=2)$ range and hence the uncertainty band for c and b

At small scales, GRV98 gives finite gluon density to much lower x than CTEQ6M

	CTEQ6M		GRV98	
ξ_R	$n_{\rm lf}=3$, $m=1.5$ **GeV**	$n_{\rm lf}=4$, $m=4.75$ **GeV**	$n_{\rm lf}=3$, $m=1.5$ **GeV**	$n_{\rm lf}=4$, $m=4.75$ **GeV**
0.5	**0.6688**	**0.2822**	**0.3312**	**0.2183**
1	**0.3527**	**0.2166**	**0.2337**	**0.1781**
2	**0.2547**	**0.1804**	**0.1840**	**0.1511**

Table 1: The values of α_s for charm and bottom production at the given values of $\xi_R=\mu_R/m$.

	CTEQ6M	GRV98
Q	$\sigma_{c\bar{c}}^{\rm NLO_{n_{lf}}}$ (μb)	$\sigma_{b\bar{b}}^{\rm NLO_{n_{lf}}}$ (μb)
c	301^{+1000}_{-210}	178^{+300}_{-122}
b	$2.06^{+1.25}_{-0.81}$	$1.65^{+0.77}_{-0.53}$

Table 2: The uncertainty on the charm and bottom total cross sections calculated from the NLO parton total cross sections.

Differences In FONLL and NLO Total Cross Sections

- FONLL total cross section obtained from integral over the p_T and y distributions; NLO total cross sections obtained from partonic total cross sections
- In FONLL, $\alpha_s(\xi_R m_T)$ and p_T is relevant scale – α_s decreases with p_T; at NLO, $\alpha_s(\xi_R m)$ and m is relevant scale, α_s is constant: fixing α_s scale in FONLL increases cross section $\sim 20 - 10\%$ for charm and bottom
- In FONLL, 'heavy' quark is considered to be a 'light' active flavor for $p_T >> m$, fixed order calculation modified to include 'massless' part of massive cross section, changes number of flavors from $n_{\rm lf}$ to $n_{\rm lf} + 1$, e.g. from 3 to 4 light flavors for charm both in FONLL and in NLO (fixed order) mode; at NLO 'heavy' quark is heavy, use $n_{\rm lf}$
- Changing the number of light flavors used in FONLL to those used in NLO, the uncertainty at $\sqrt{S} = 200$ GeV is the same both cases
- Largest differences in two approaches for charm; bottom results less affected by changes in $n_{\rm lf}$, scale, parton density

Which is Right??
OR
IS There a Right Answer for Charm??

- **NLO is presumably right treatment if you could just sit and count produced charm quarks, closest to fixed-target measurements where p_T is typically low, $p_T \sim m$ or $p_T < m$**
- **At collider energies where only high p_T c and b are detected, charm mass is irrelevant with respect to p_T and FONLL is clearly right choice**
- **At colliders where full range of p_T can be measured, e.g. STAR can reconstruct low p_T D^0, less clear at low p_T but FONLL approach more correct at high p_T**
- **Choice of number of light flavors most important since it affects value of α_s strongly**
- **Low x, low scale behavior of gluon density is almost as important as number of light flavors – obviously this won't be settled until there are better determinations of gluon density available in this relevant region**
- **No good 'RIGHT' answer, means little predictive power for charm total cross section**

PYTHIA vs. NLO Calculations

PYTHIA **requires separate calculations depending on how many heavy quarks at hard vertex, labeled pair creation (2), flavor excitation (1) and gluon splitting (0) rather than grouping diagrams by initial state as in NLO ($q\overline{q}$, gg, qg)**

Splitting and excitation are subclasses of gg and qg NLO diagrams

PYTHIA **typically gives larger cross sections because no interference terms**

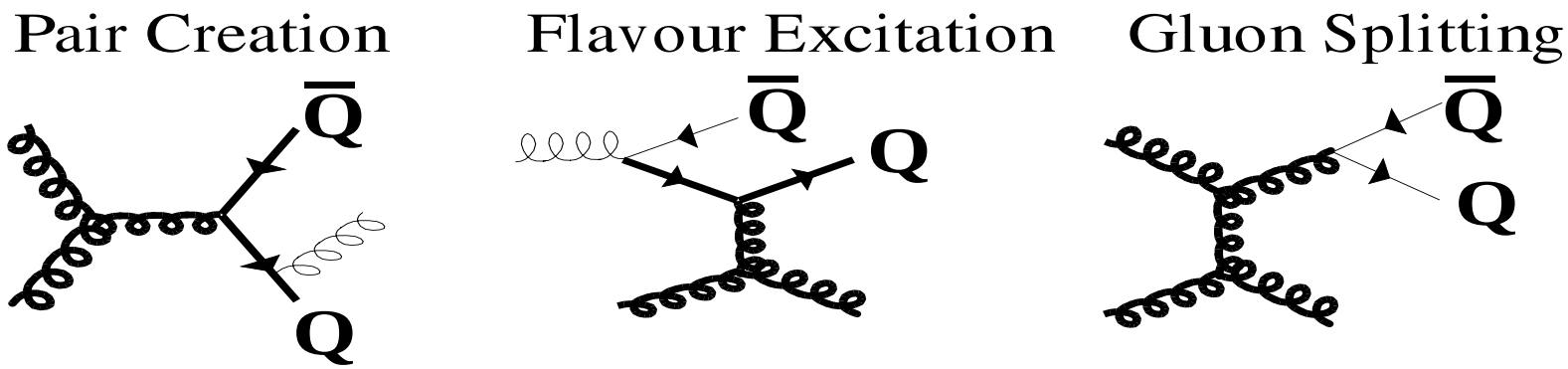

Figure 16: Examples of pair creation, flavor excitation and gluon splitting. The thick lines correspond to the hard process, the thin ones to the parton shower.

Production Properties in PYTHIA

<u>Pair creation:</u> **Two heavy quarks in hard scattering**

LO diagrams and (multiple) virtual gluon emission

$Q^2 = m^2 + \hat{p}_\perp$, **massive matrix elements**

<u>Flavor excitation:</u> **Heavy flavor from parton distribution of beams,** $Qq \to Qq$, $Qg \to Qg$

One heavy quark in hard scattering

If Q **is not a valence quark, must be generated from** $g \to Q\overline{Q}$

$Q^2 = \hat{p}_\perp^2 = \hat{t}\hat{u}/\hat{s}$

Since $f_Q^p = 0$ **for** $Q^2 < m^2$, **massless matrix elements used**

<u>Gluon splitting:</u> $g \to Q\overline{Q}$ **in initial or final state shower, no** Q **in hard scattering**

Space-like shower: $Q^2_{\rm max} = Q^2 = m^2\,(\text{threshold})$

Time-like shower: $M^2_{\rm max} = 4Q^2 = 4m^2\,(\text{threshold})$

Parameters CTEQ 5L, $m_c = 1.5$ **GeV,** $m_b = 4.8$ **GeV,** $\Lambda_4 = 0.192$ **GeV**

Total Charm $\sqrt{S}$ Dependence in PYTHIA Similar to NLO

The trend of the total charm cross section with energy is similar to NLO but, for same parameters, PYTHIA tends to give higher cross section

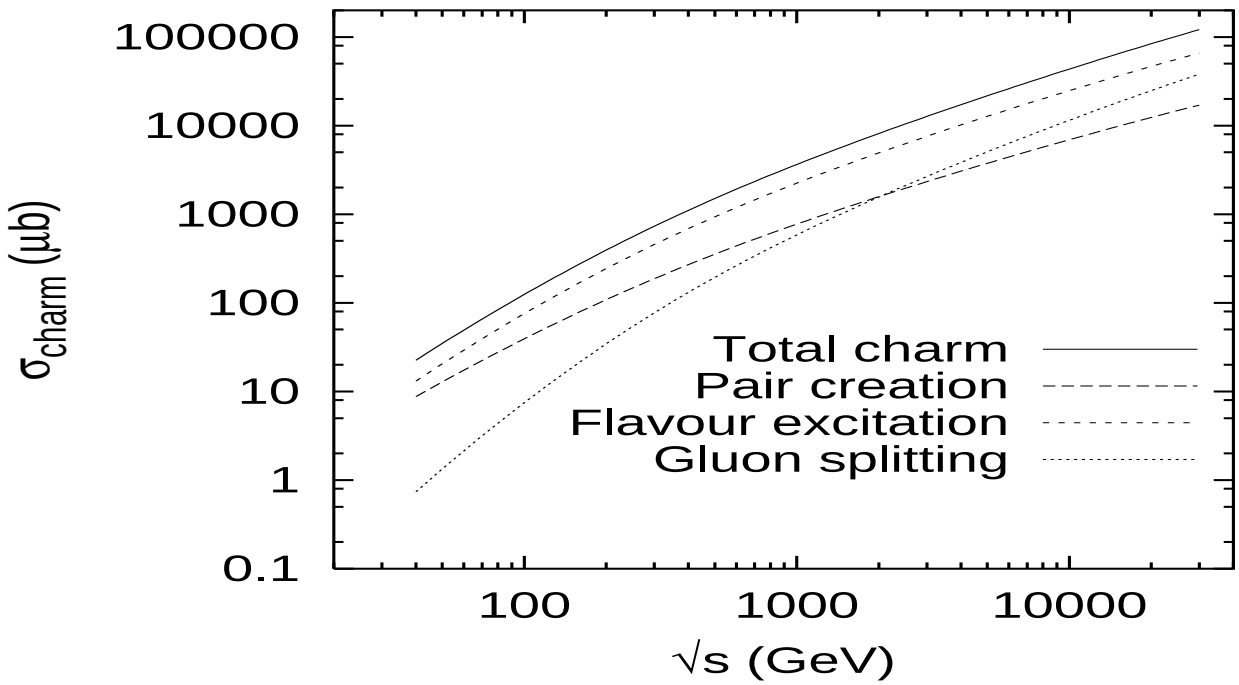

Figure 17: The total charm cross section in pp interactions with PYTHIA is shown as a function of energy. The long-dashed line is the pair creation contribution, the short-dashed line, flavor excitation, and the dotted line, gluon splitting. The sum of the three contributions is given by the solid line. From Norrbin and Sjostrand, Eur. J. Phys. **C17** (2000) 137.

At LO Level, Distributions Nearly Identical

Parton showers turned off in PYTHIA and k_T kick, $\langle k_T^2 \rangle = 1$ GeV^2, included in PYTHIA and LO calculations – without k_T kick, LO calculation would be a delta function

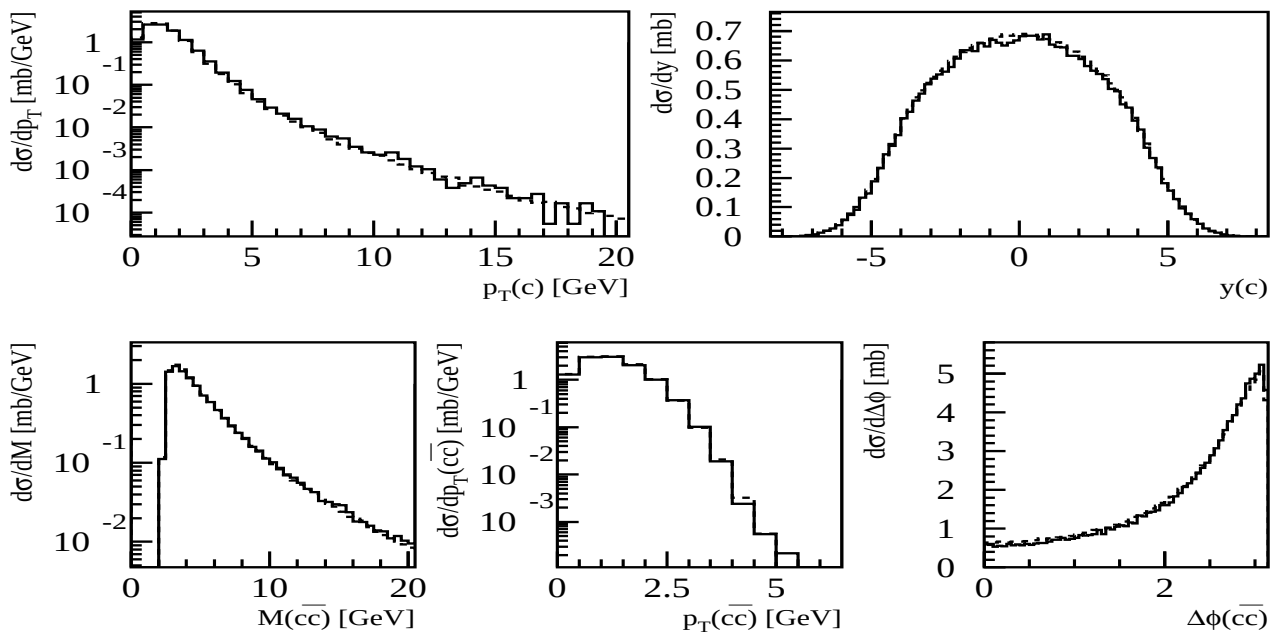

Figure 18: Comparison between PYTHIA results (solid histogram) for $gg \to c\bar{c}$, without parton showers, and the MNR calculation (Nucl. Phys. B **405** (1993) 507) of the same process at LO (dashed histogram) at $\sqrt{S} = 5.5$ TeV. From arXiv:hep-ph/0311048.

PYTHIA Parameters Used to Compare to NLO

description	parameter	Charm	Bottom
Process types	MSEL	1	1
Quark mass	PMAS(4/5,1)	1.2	4.75
Minimum $p_T^{\rm hard}$	CKIN(3)	2.1	2.75
CTEQ4L	MSTP(51)	4032	4032
Proton PDF	MSTP(52)	2	2
No multiple	MSTP(81)	0	0
interactions	PARP(81/82)	0	0
Parton showers on	MSTP(61/71)	1	1
2$^{\rm nd}$ order α_s	MSTP(2)	2	2
QCD scales	MSTP(32)	2	2
for hard scattering	PARP(34/67)	1	1
and parton shower	PARP(71)	4	1
	MSTP(91)	1	1
	PARP(91)	1.304 (Pb+Pb)	2.035 (Pb+Pb)
Intrinsic k_T		1 (pp)	1 (pp)
	PARP(93)	6.52 (Pb+Pb)	10.17 (Pb+Pb)
		5 (pp)	5 (pp)

Table 3: PYTHIA parameters for c and b production in Pb+Pb collisions at $\sqrt{S_{NN}} = 5.5$ TeV and pp collisions at $\sqrt{S} = 14$ TeV. Unspecified parameters are PYTHIA 6.150 defaults.

Charm Distributions: NLO vs. PYTHIA

Agreement gnerally rather good, PYTHIA $\Delta\phi$ distribution peaked more toward π than NLO

'Flavor excitation' and 'gluon splitting' more isotropic (3-body final states) while 'flavor creation' is more back-to-back
k_T kick has biggest effect on $\Delta\phi$ distribution

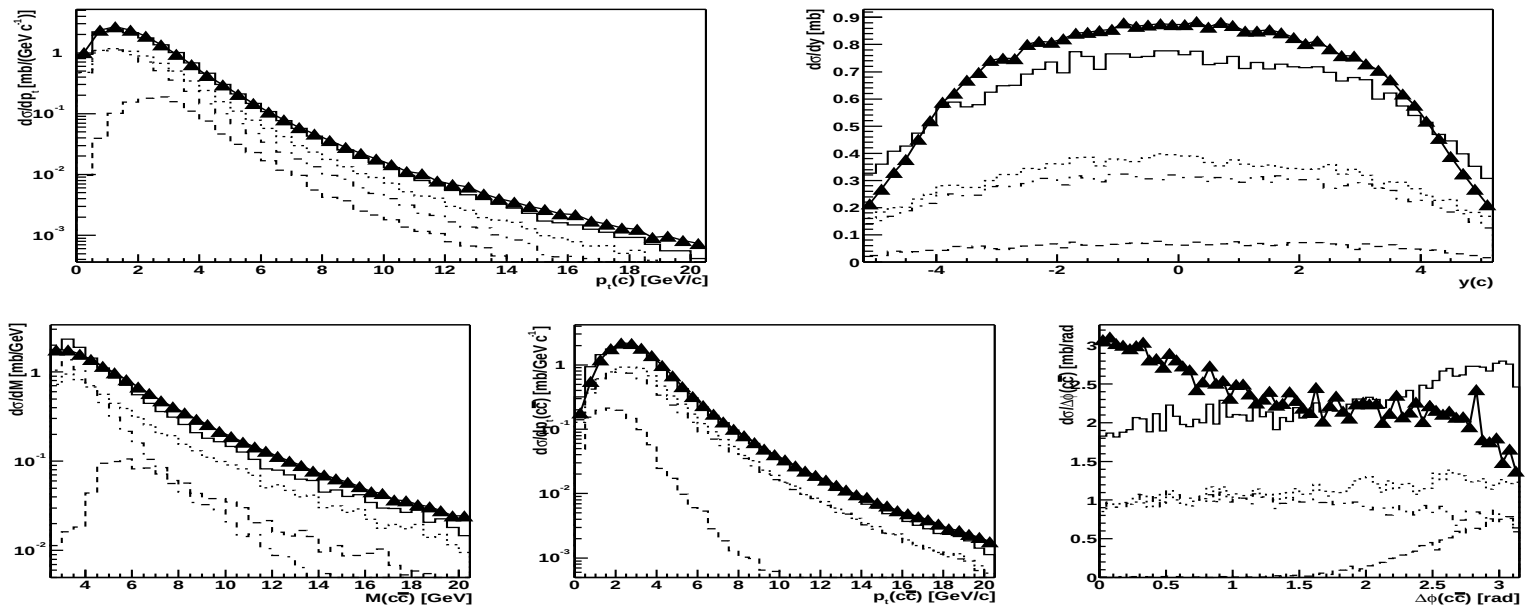

Figure 19: Comparison between charm production in the NLO calculation by Mangano, Nason and Ridolfi and in PYTHIA with parameters tuned as described in the text for Pb+Pb collisions at $\sqrt{S_{NN}} = 5.5$ TeV. The triangles show the NLO calculation, the solid histogram corresponds to the PYTHIA total production. The individual PYTHIA contributions are flavor creation (dashed), flavour excitation (dotted) and gluon splitting (dot-dashed). From arXiv:hep-ph/0311048.

Total Bottom $\sqrt{S}$ Dependence Similar to NLO

'Creation' processes dominate bottom production to above RHIC energies
Another way of saying 'bottom production has a lower K factor'

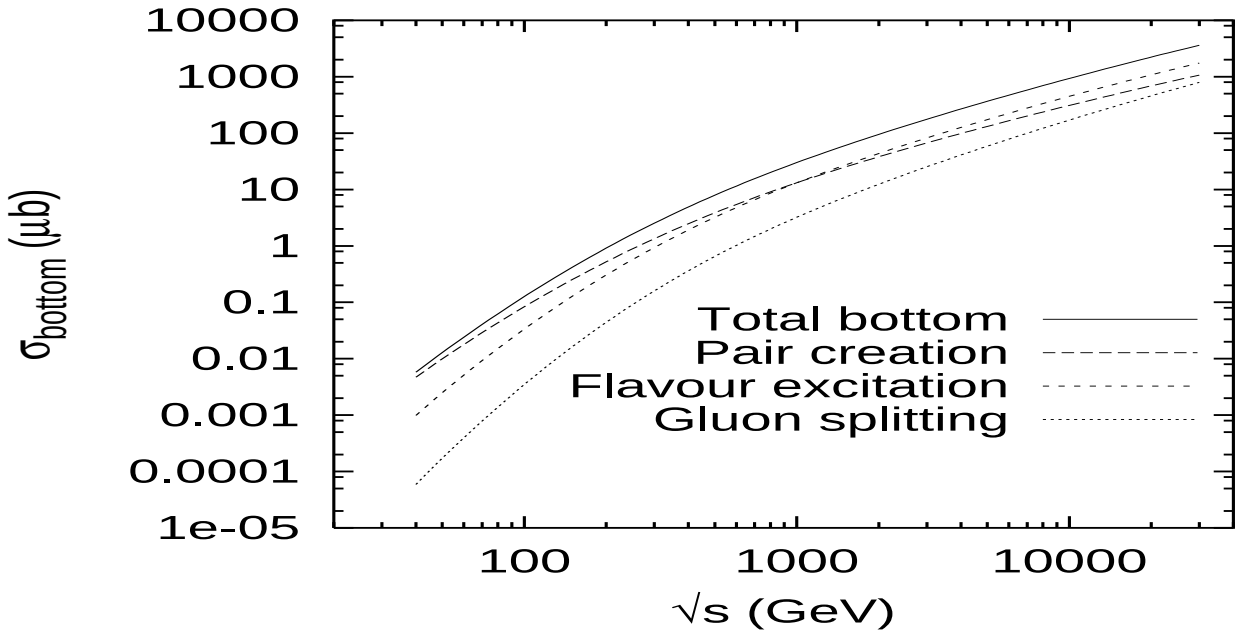

Figure 20: The total bottom cross section in pp interactions with PYTHIA is shown as a function of energy. The long-dashed line is the pair creation contribution, the short-dashed line, flavor excitation, and the dotted line, gluon splitting. The sum of the three contributions is given by the solid line. From Norrbin and Sjostrand, Eur. J. Phys. **C17** (2000) 137.

Bottom Distributions: NLO vs. PYTHIA

Azimuthal distribution for bottom production more 'back-to-back' for both NLO and PYTHIA

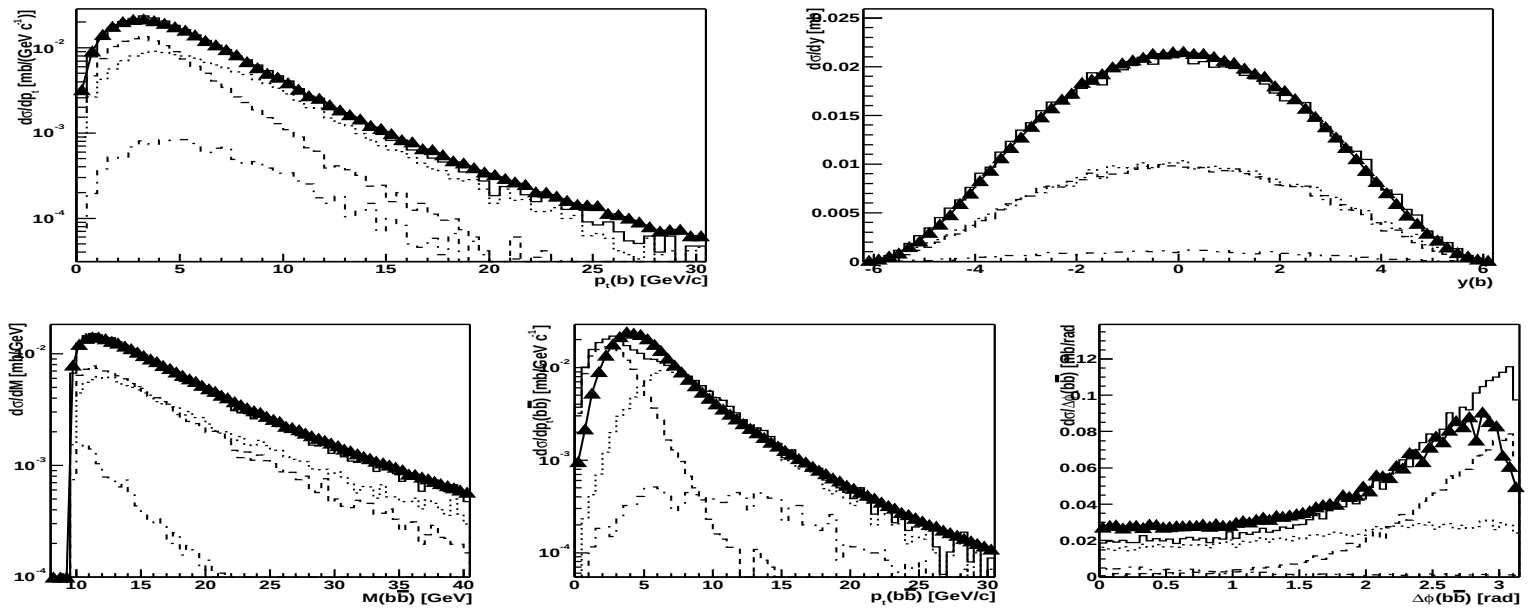

Figure 21: Comparison between bottom production in the NLO calculation by Mangano, Nason and Ridolfi and in PYTHIA with parameters tuned as described in the text for Pb+Pb collisions at $\sqrt{S_{NN}} = 5.5$ TeV. The triangles show the NLO calculation, the solid histogram corresponds to the PYTHIA total production. The individual PYTHIA contributions are flavor creation (dashed), flavour excitation (dotted) and gluon splitting (dot-dashed). From arXiv:hep-ph/0311048.

Summary

- **Total charm cross sections have large theoretical uncertainties**
- **Differences between FONLL and NLO total charm cross sections hinge on number of light flavors used in calculation**
- **Uncertainty due to low x, low scale parton density is as large as those due to mass, scale and number of light flavors – can't be eliminated until more measurements available in relevant region**
- **More massive bottom quarks behave better**
- **PYTHIA and NLO calculations give similar $\sqrt{S}$ dependence for total charm cross sections (but PYTHIA gives higher total for same mass and scale) and same basic shape for most differential distributions but only if PYTHIA parameters tuned properly – Care needed in interpretation, not different mechanisms than NLO, just different PYTHIA implementation**